Agricultural and Forest Meteorology 153 (2012) 3–13

Contents lists available at ScienceDirect

Agricultural and Forest Meteorology

journal homepage: www.elsevier.com/locate/agrformet

Energy balance closure at the BERMS flux towers in relation to the water balance of the White Gull Creek watershed 1999–2009

A.G. Barr[a,*], G. van der Kamp[a], T.A. Black[b], J.H. McCaughey[c], Z. Nesic[b]

[a] Science and Technology Branch, Environment Canada, Canada
[b] Faculty of Land and Food Systems, U.B.C., Canada
[c] Department of Geography, Queen's U., Canada

ARTICLE INFO

Article history:
Received 4 December 2010
Received in revised form 18 April 2011
Accepted 23 May 2011

Keywords:
Surface energy balance
Water balance
Boreal forest
Energy balance closure
Streamflow
Watershed

ABSTRACT

The eddy-covariance method has become a cornerstone in the study of the surface energy and water balances, yet the oft-reported lack of energy-balance closure adds uncertainty to its measurements of evapotranspiration. This study explores the issue of closure based on 10 years of energy and water balance measurements at seven flux-tower sites in the southern boreal forests of western Canada. The sites include mature aspen, black spruce and jack pine forests, three young jack pine forests following harvesting, and one fen. Careful attention was paid to the measurement of evapotranspiration E, surface available energy (net radiation minus storage), precipitation P, and soil water storage S including root-zone soil water and water table elevation. Stand-level outflow O at the flux-tower sites was estimated annually as a residual term in the vertical water balance ($O = P - E - \Delta S$), with and without energy-closure adjustments to E. Six of the flux towers were located within or near the gauged White Gull Creek watershed (603 km^2). The comparison of measured streamflow from the White Gull Creek with estimated outflow, scaled from the flux towers to the watershed, provides an independent test of the need for energy-closure adjustments to flux-tower E.

Measured streamflow from the White Gull Creek watershed had a long-term mean (S.D.) of 101 (54) mm y^{-1} but was highly variable among years, ranging from 30 mm y^{-1} during an extreme dry year to 204 mm y^{-1} during an extreme wet year. Stand-level outflow, estimated with an energy-closure adjustment to E, varied by land-cover type, from a mean (S.D.) of 30 (35) mm y^{-1} at the mature aspen forest and 52 (125) mm y^{-1} at the fen to 108 (85) mm y^{-1} at the mature black spruce forest and 187 (55) and 250 (64) mm y^{-1} at the mature and young (harvested) jack pine forests, respectively. The dominant land-cover type, mature black spruce forest, typified the hydrology of the boreal forest landscape, with outflow similar to the watershed mean.

The warm-season, eddy-covariance sensible and latent heat fluxes were 15 ± 4% (annual mean ± S.D.) smaller than surface available energy, with reasonable similarity among sites and years. When scaled from stand to watershed, the tower-based estimates of outflow agreed with measured streamflow only when outflow was calculated with an energy-closure adjustment to E. The annual means for the 2002–2009 hydrologic years were: 131 mm y^{-1} (measured streamflow); 182 mm y^{-1} (tower-based outflow calculated without energy-closure adjustments to E); and 112 and 127 mm y^{-1} (tower-based outflow calculated with energy-closure adjustments to E from two different schemes). This result corroborates the need for energy-closure adjustments to eddy-covariance measurements of E, but it does not provide guidance about how the adjustments should be implemented.

1. Introduction

The boreal forest plays an important role in the earth's hydrologic cycle. The boreal forest is a mosaic of contrasting land-cover types resulting from the interplay of topography, drainage, soil water holding capacity, disturbance history and ecological succession. The spatial pattern of its climax vegetation is controlled by soil drainage and available soil moisture, with peatlands in the poorly drained deeper depressions, black spruce forests and treed wetlands in the more subtle lowland depressions, jack pine forests on the well-drained sandy uplands, and mixedwood and aspen forests on the well-drained loamy uplands. Superimposed is the spatial pattern of disturbance history. Fire is the dominant disturbance regime (Landsberg and Gower, 1997), with a return period

* Corresponding author.
E-mail address: alan.barr@ec.gc.ca (A.G. Barr).

0168-1923/$ – see front matter © 2012 A.G. Barr. Published by Elsevier B.V. All rights reserved.
doi:10.1016/j.agrformet.2011.05.017

of 50–200 years (Bonan and Shugart, 1989). Harvesting plays a less important role because of the boreal forest's low productivity (Landsberg and Gower, 1997). The ecozone has a long cold season, a short growing season and frequent forest fires. At the southern edge, the transitional aspen parklands border on the grasslands to the south. The forest–grassland ecotone is controlled by the water balance, with precipitation exceeding potential evapotranspiration to the north and potential evapotranspiration exceeding precipitation to the south (Hogg, 1997).

The Boreal Plains ecozone of western Canada is a nearly level to gently rolling plain with hummocky to kettled glacial moraine and lacustrine deposits. The surface materials are usually deep and the soils are relatively fertile. The water cycle of the Boreal Plains ecozone is characterized by a moderately small excess of water (precipitation minus evapotranspiration) in most years, low outflow with high seasonal and interannual variability, a significant winter snowpack, and large runoff during spring snowmelt and in summers with high rainfall. The subtle topographic relief and heterogeneous land-cover types of the Boreal Plains landscape make it hydrologically complex, with fundamental differences in the hydrologic functioning of its upland, lowland and wetland ecosystems (Devito et al., 2005). The role of the Boreal Plains' diverse land-cover types in the hydrologic cycle are not well documented, nor are the hydrologic responses to climate change.

Ecohydrological studies at flux towers are providing new insights into the coupling of the water and carbon cycles in northern ecosystems (Grant, 2004; Ju et al., 2006). At millennial time scales, carbon accumulates in the poorly drained depressions of peatlands and treed wetlands. The spatial distribution of land-cover types and their associated carbon stocks is influenced by soil drainage and soil texture. Hydrology links these land-cover types across the diverse and heterogeneous boreal landscape.

Precipitation and evapotranspiration are dominant terms in the water cycle. Because flux-tower networks measure the surface energy and vertical water balances, including evapotranspiration, they have the potential to contribute to advances in hydrology and hydrological modelling. This potential is just beginning to be realized, due in part to the growing length of the flux tower time series and the growing focus on water cycle measurements at flux tower sites and in their catchments. In turn, associated hydrologic measurements can shed light on flux-tower measurements, including the contentious issue of energy-balance closure (Barr et al., 2000; Scott, 2010; Wohlfahrt et al., 2010).

Eddy-covariance studies often report an imbalance between the surface available energy (net radiation minus the surface energy storage fluxes) and the sum of the sensible and latent heat fluxes (Aubinet et al., 2000; Wilson et al., 2002; Li et al., 2005; Barr et al., 2001, 2006; Oncley et al., 2007; Foken et al., 2010). The expectation that the energy-closure problem would be resolved by improvements in eddy-covariance instrumentation and software has not been fulfilled, suggesting that the cause is meteorological rather than instrumental (Foken, 2008). The energy imbalance introduces a serious systematic error in evapotranspiration that must be addressed before the data are used in water balance studies (Wohlfahrt et al., 2010) or in the evaluation and development of land surface process models (Williams et al., 2009). Hydrologic studies have the potential to clarify the energy-closure issue, because streamflow measurements provide an independent check on water balance closure (and thus on evapotranspiration) at the catchment scale (Wilson et al., 2001; Scott, 2010).

This study reports energy and water balance measurements over 10 hydrologic years at seven flux-tower sites in the Boreal Ecosystem Research and Monitoring Sites (BERMS) network in central Saskatchewan, Canada. The sites include one wetland, mature aspen, black spruce and jack pine forests, and three younger jack pine stands following harvesting. The study period includes a severe three-year drought followed by three years of extreme high precipitation. The objective was to evaluate the importance of energy-closure adjustments to evapotranspiration by comparing local, stand-level estimates of lateral outflow, inferred from the vertical water balance at eddy-covariance flux towers, with watershed-scale measurements of streamflow.

2. Water and energy balances

The vertical water balance may be written as

$$P = E + \Delta S + O \tag{1}$$

where P and E are the rates of precipitation and evapotranspiration, ΔS is the rate of change of water storage in the soil and snowpack, and O is the rate of lateral outflow from overland runoff, interflow and groundwater baseflow combined. Typical units for the variables in (1) are ($\mathrm{mm\,d^{-1}}$) or ($\mathrm{mm\,y^{-1}}$). At the stand scale, P, E and ΔS can be measured directly and O calculated as a residual. At the watershed scale, outflow can be measured directly via streamflow, which we denote as F, or indirectly by scaling the stand-level estimates of O to the watershed, which we will denote as $\bar{O}$ (Section 3.3.4). Although it is not feasible to compare stand-based estimates of watershed outflow $\bar{O}$ with measured F over short time scales (hours or days) because of temporal lags in horizontal water transport, the values can be compared at the annual time scale for which changes of water storage in the watershed are typically less important in the water balance. The comparison of annual O, $\bar{O}$ and F is best done over the hydrologic year (autumn to autumn), when the measurement of ΔS is not complicated by the presence of a snowpack or the freezing of soil water and the streamflow values are typically small and steady.

The surface energy balance may be written as

$$R_n = H + \lambda E + Q \tag{2a}$$

where R_n is the net radiation flux density, H is the surface sensible heat flux density including storage changes in the air layer below the flux measurement (Barr et al., 2006), λE is the surface latent heat flux density including storage, and Q is the sum of the surface energy storage fluxes. Typical units for the variables in (2a) are ($\mathrm{W\,m^{-2}}$). The Q term as measured in this study pertains to the warm season only. It includes: Q_g the soil heat flux density; Q_b the rate of change of heat storage in the above-ground biomass; and Q_p the energy flux density associated with the CO_2 flux (through photosynthesis and respiration). It does not include terms for freeze–thaw events or heat storage in the snow pack, neither of which were measured.

Energy imbalances (ε) occur in flux-tower studies when the sum of the eddy-covariance sensible and latent heat fluxes does not equal surface available energy (net radiation minus surface storage fluxes), so that

$$R_n = H + \lambda E + Q + \varepsilon \tag{2b}$$

The energy-closure fraction CF is defined as:

$$\mathrm{CF} = \frac{(H + \lambda E)}{(R_n - Q)} = 1 - \frac{\varepsilon}{(R_n - Q)} \tag{3}$$

where values of CF below one indicate a flux measurement deficit.

3. Sites and measurements

3.1. Study area

The BERMS study area is located near the southern edge of the boreal forest in the Boreal Plains ecozone, just to the north of Prince Albert, Saskatchewan (Fig. 1). The study area includes seven flux towers in representative land-cover types (Table 1). In the eastern portion of the BERMS study area is the White Gull Creek

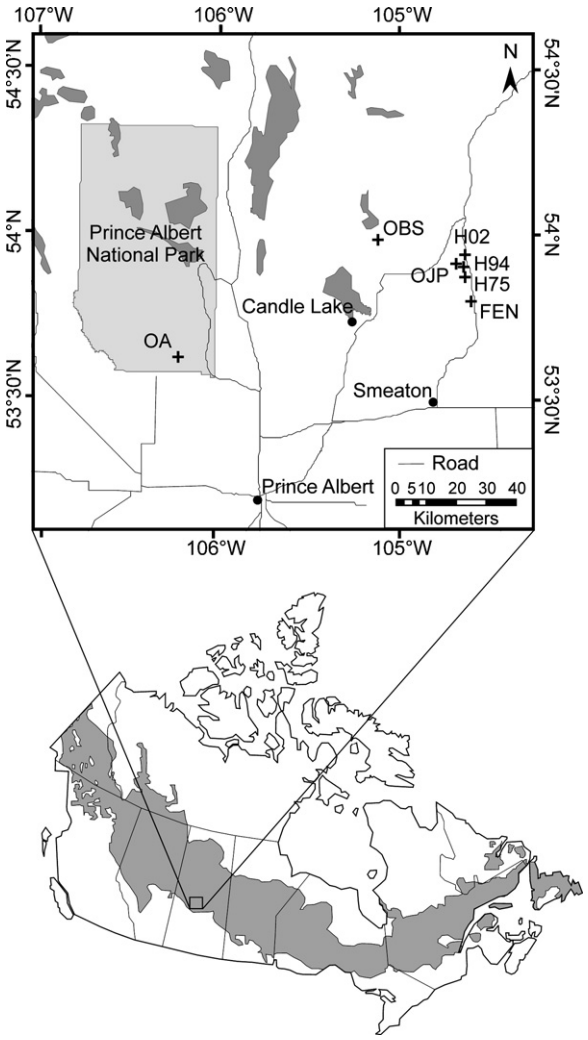

Fig. 1. Study area, showing the Canadian boreal forest (lower panel, shaded) and location of the flux towers (+) (upper panel).

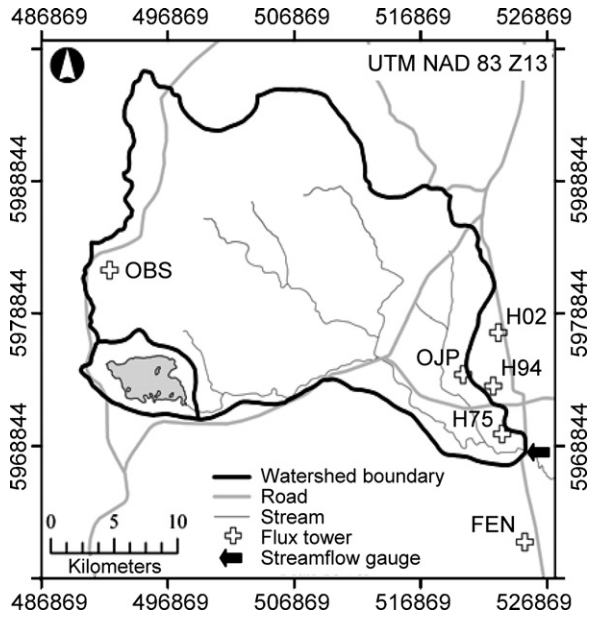

Fig. 2. UTM coordinates of the White Gull Creek watershed, showing the location of the flux towers (+), the streamflow gauging station (arrow), and the White Gull Lake sub-basin (southwest corner).

watershed, with a gross drainage basin drainage area of 629 km^2 and an estimated effective drainage area of 603 km^2 (Fig. 2). During the entire 1999–2009 study period, the White Gull Lake sub-basin, about 26 km^2, was not hydrologically connected to White Gull Creek due to the low water level of the lake, and therefore this part of the watershed has been excluded for the purpose of water balance estimates. White Gull Creek has been gauged for continuous streamflow measurement since 1993 (Nijssen and Lettenmaier, 2002). Flow data area available on the Water Survey of Canada website (http://www.wsc.ec.gc.ca/applications/H2O/index-eng.cfm). In the general vicinity of the gauge, the horizontal hydraulic gradient of the Creek is about 0.003 as estimated from the topographic map of the area. The mean (S.D.) annual streamflow for the October–September hydrologic year, 1993–2009, was 101 (54) mm y^{-1}.

Table 1
Flux-tower site characteristics.

Site Name	Old Aspen	Old Black Spruce	Old Jack Pine	Harvested Jack Pine 1975, 1994, 2002			Fen
Abbreviation	OA	OBS	OJP	H75	H94	H02	Fen
Latitude (°N)	53.63	53.98	53.92	53.88	53.91	53.94	53.78
Longitude (°W)	106.20	105.12	104.69	104.69	104.69	104.69	104.69
Canopy height (m, 2002)	21	16	10	7.6	1.7	n/a	n/a
Leaf area index	3.9–5.2[a]	3.0	2.0	3.1	0.8	0.3	n/a
Flux measurement height (m)	39	28	24	16	5	2	4
Flux measurement period	April 1996+	April 1999+	September 1999+	April 2004–September 2009	April 2000–December 2006	April 2003–August 2008	April 2002+
Stand history	Fire 1919	Fire ~1879	Fire 1914	Clearcutting 1975, 1994, 2002			~6,000 BC[b]
Land-cover fraction, White Gull Creek watershed[c]	0.18	0.39	0.18			0.11	0.14
References	Black et al. (1996), Barr et al. (2006)	Barr et al. (2006)	Barr et al. (2006)	Zha et al. (2009), Kidston et al. (2010)			Hogan et al. (2006), Sonnentag et al. (2009)

[a] Growing-season maximum.
[b] Mid-Holocene cooling.
[c] Abstracted from Nijssen and Lettenmaier (2002).

The physical setting of the BERMS area, including the White Gull Creek watershed, is described in detail by Judd-Henrey et al. (2008). van der Kamp and Hayashi (2009) give a general overview of the hydrogeology and groundwater flow in the glacial deposits of the northern interior plains of North America. The White Gull Creek watershed and its surroundings are underlain by 100–200 m of glacial deposits, consisting largely of clay-rich glacial till, interspersed with thin and discontinuous sand and gravel layers. The thick layers of low-permeability glacial till preclude any significant groundwater exchange of surface water and shallow groundwater with deeper intertill aquifers and underlying bedrock aquifers. The surficial geology of the western portion of the watershed is described as "Moraine Plain", predominantly glacial till. Tributaries of White Gull Creek in this portion of the watershed had little or no flow in October 2003 at the end of a long drought because groundwater flow to the streams through the surficial till is very slow.

The eastern portion of the watershed is classed as "Glaciofluvial Plain" generally having sand and gravel outwash deposits at the surface with a total thickness of 10–15 m. At higher elevations, the water table lies 5–10 m below the ground surface. This portion of the watershed exhibited significant groundwater-fed baseflow in October 2003, emanating from the permeable surficial aquifers. The watershed boundary along the east side is in the form of a groundwater divide within the surficial aquifer. The boundary location (Fig. 2) is estimated on the basis of the topography and the location of surface streams and springs. In accordance with the estimated location of the groundwater divide, the groundwater flow at the Old Jack Pine (OJP) site (Fig. 2) was directed toward White Gull Creek throughout the study period, as evidenced by the recorded water levels in a triangular arrangement of observation wells at the site. In view of the low topographic gradients, the shallow depth of the surficial aquifer, and the discontinuous nature of the deeper confined aquifer zones, groundwater flow beneath the watershed boundaries and the gauge location is assumed to be negligible compared to the streamflow. The upland vegetation in the watershed reflects the surficial geology, with predominantly black spruce mixed with aspen in the west and jack pine in the east.

The climate of the study area is continental with a long and dry cold season and a short growing season. The 1971–2000 climate normals from Waskesiu Lake (53.92°N, 106.07°W, www.climate.weatheroffice.gc.ca) report mean annual, January and July air temperatures of 0.4, −17.9 and 16.2 °C, respectively, and mean annual precipitation of 467 mm, 30% of which fell as snow.

3.2. Flux-tower sites

The flux-tower sites include three mature forest stands, three younger forest stands following harvesting, and one wetland (Table 1). Five of the sites were established in 1994 as part of the Boreal Ecosystem–Atmosphere Study (BOREAS, Sellers et al., 1997) and have continued since 1997 as part of the BERMS and Fluxnet-Canada networks. The two younger sites, harvested in 1994 and 2002, were established in 2000 and 2003, respectively. Table 1 summarizes the salient site characteristics. The seven flux towers span the full spectrum of land-cover types in the White Gull Creek. Three of the flux towers (OBS, OJP and H75) are located within the watershed; three others (H94, H02 and Fen) lie just outside its boundaries. The OA flux tower, located ~80 km to the southwest, is typical of the watershed's aspen and mixedwood forests.

The Old Aspen (OA) site in Prince Albert National Park has a trembling aspen overstory (*Populous tremuloides* L. with scattered *Populous balsamifera* L.) and hazel understory (*Corylus cornula* Marsh.). The subsurface geology consists of clay-rich glacial till, below 10-cm LFH and 30-cm silt loam mineral soil horizons. The water table lies from 1 to 5 m below the ground surface, varying spatially due to the hummocky terrain and varying in time in response to variations in precipitation. A small depression near the tower was inundated during the wettest years.

The Old Black Spruce (OBS) site is dominated by black spruce (*Picea mariana* Mill. BSP), with sparsely distributed tamarack (*Larix laricina* Du Roi, 10%) and a sparse understorey of shrubs (e.g., *Ledum groenlandicum* Retzius and *Vaccinium vitisidaea* L.) and feather moss (*Hylocomium splendens*, *Pleurozium schreberi*), with irregular patches of hummocky peat (*Sphagnum* spp.) and lichen (*Cladina* spp.) in wetter and drier areas, respectively. The soil has an approximately 20-cm deep peat layer overlying waterlogged sand, with imperfect to poor drainage and the depth to the water table varying between 0 and 1 m below the ground surface.

The OJP and three post-harvest jack pine sites are located within 5 km of each other in flat portions of a glacial outwash plain. The harvested stands regenerated following clearcut harvesting in 1975 (H75), 1994 (H94) and 2002 (H02). The overstories are pure stands of jack pine (*Pinus banksiana* Lamb.). The understories are mixtures of reindeer lichen (*Cladonin* spp.) at OJP, bearberry (*Arctostaphylos uva-ursi* (L.) Spreng) at the harvested sites, and infrequent, scattered clumps of green alder (*Alnus viridis* spp. *crispa* (Ait.) Turrill) co-occurring with feathermoss (*Pleurozium* spp.). At all four jack pine sites, the sandy soil is nutrient poor and well drained with the water table lying at least 5 m below the ground surface.

The Fen site is a minerotrophic patterned fen surrounded by black spruce and jack pine forests. The depth of the peat varies from 2 to 3 m in the center to 1 m near the edges. The dominant herbaceous plants are buckbean (*Menyanthes trifoliate*) and several sedge species (*Carex* and *Eriophorum* spp.). The dominant woody species are scattered bog birch (*Betula pumila*) and tamarack (*L. laricina* (Du Roi) K. Koch). The water table is generally at or above the peat surface except in very dry years.

3.3. Measurements

3.3.1. Meteorology

Air temperature was measured at each site using temperature/humidity probes (model HMP45C, Vaisala Inc., Oy, Finland) mounted in radiation shields above the canopy. Precipitation was measured at OA, OBS, OJP and Fen using an accumulating gauge (Belfort model, 3000 with an Alter shield, Belfort Instruments, Baltimore, MD, USA), with motor oil added to prevent water losses by evaporation and antifreeze added to prevent freezing. At the three forest sites, the gauges were situated in the center of small forest clearings, at approximately one tree height from the clearing edges, to optimize snow catch efficiency. At the fen, the gauge was located in the open. Snowfall was corrected for wind-induced undercatch based on the catch efficiency CE, estimated daily from measured windspeed u at gauge height (Goodison, 1978):

$$\mathrm{CE} = \exp(-0.0055 - 0.133u) \quad (4)$$

At the three forest sites, the snowfall corrections were small, increasing annual P by less than 1%. At the Fen, which was not sheltered from the wind, the snowfall correction increased annual P by an average of 9%.

3.3.2. Soil water and water table depth

The soil volumetric water content θ was measured at OA using time domain reflectometry (Moisture Point Type B segmented probes, ESI, Victoria, Canada, mean of three profiles at 0–15, 15–30, 30–60, 60–90, and 90–120 cm depth). At the other sites, θ was measured using soil moisture reflectometers (model CS615, Campbell Scientific, Logan, USA, mean of two profiles) at depths of 2.5, 7.5, 22.5 and 45 cm, inserted horizontally, and 60–90 cm, inserted vertically, at OBS, and 0–15, 15–30, 30–60, 60–90, 90–120 and 120–150 cm depth at the jack pine sites. Water table depth was monitored using pressure transducers (model Druck PDCR, 1230,

Table 2
Soil properties used in Eq. (5).

Site	z_{rz} (m)	Porosity[a] (θ_{sat})	Observed θ_{fc}[b]	$\theta_{sat} - \theta_{fc}$
OA	1.2	0.45 (Ck)	0.35 (90–120 cm)	0.10
OBS	0.6	0.37 (Bt)	0.30 (60–90 cm)	0.07
OJP, H75, H94, H02	2.5	0.43 (C)	0.13 (120–150 cm)	0.30

[a] Estimated from the bulk density of the relevant soil horizon (shown in the brackets).
[b] Estimated as the 95th percentile of measured soil volumetric water content in the warm season.

GE Sensing, Billerica, MA, USA at OA and OBS, and Levelogger model 3001, Solinst Canada Ltd., Georgetown, ON, Canada at all other sites). The water table measurement was within the flux footprint at all sites but OA, where it was in a similar aspen stand located 1.3 km east of the flux tower. The water table measurements spanned the study period at OA and OBS but began in 2002 at all other sites.

The annual change in soil water storage ΔS was estimated at all sites but the Fen from measurements of soil water, integrated through the root zone, and water table depth as

$$\Delta S = z_{rz}\Delta\theta_{rz} + (\theta_{sat} - \theta_{fc})\Delta z_{wt} = \Delta S_{rz} + \Delta S_{wt} \quad (5)$$

where z_{rz} is the depth of the root zone, z_{wt} is the water table depth, and θ is the soil volumetric water content in the root zone (θ_{rz}), at saturation below the water table (θ_{sat}), and at field capacity just above the water table (θ_{fc}) (Table 2). Eq. (5) includes two terms: ΔS_{rz} – the change in soil water storage in the root zone; and ΔS_{wt} – the change in soil water storage associated with a rising or falling water table, estimated as the product of the change of water table depth and the associated change in θ, i.e., $\theta_{sat} - \theta_{fc}$ (Table 2). θ_{sat} was estimated from the porosity whereas θ_{fc} was inferred from the measured θ time series at the bottom of the root zone. Eq. (5) assumes that the layer between the root zone and the water table remains at field capacity. When the water table impinged on the root zone, the water table depth was set to the root-zone depth to avoid double counting. At OJP only, where the root zone extended below the soil water measurements to 2.5 m, we used the θ value from 1.2 to 1.5 m to represent the layer from 1.5 to 2.5 m.

The changes in water storage at the Fen were based on continuous records of water table elevation at two locations on opposite sides of the flux tower, and on the elevation of the peat surface, measured with bog shoes at the same locations as the water table measurements (Hogan, 2005). The absolute water table elevation was determined with respect to steel piezometer pipes anchored in the sand substrate beneath the peat, because the peat surface itself was subject to vertical movements of up to 0.40 m associated with changes in the water table. The elevations of these "benchmark" piezometers were surveyed relative to a fixed geodetic datum (Geodetic Survey of Canada Benchmark # 65S187). They were repeatedly surveyed relative to each other and to the deeply anchored flux tower, to verify that there were no significant vertical movements of the piezometers. Water storage S at any point in time was determined from the absolute water table elevation z (relative to the reference geodetic elevation) and from the height of the water table w relative to the peat surface (positive when the water table was above the peat surface)

$$S = \begin{cases} z; w \geq 0 \\ z + p[w - z_m(1 - z_m \exp(w/z_m))]; w < 0 \end{cases} \quad (6)$$

where S is the water storage relative to a reference water table at $z = 0$, p is the porosity of the peat at the average peat surface ($p \sim 0.95$ for the Fen), and z_m is a characteristic depth, determined from in situ water yield tests to equal 0.147 m for the Fen. Eq. (6) includes a correction for water retention above the water table when the water table dropped below the peat surface (Hogan et al., 2006). The correction reflects the fact that the more decomposed peat at depth has small pore spaces and high water retention capacity. The annual calculation of the Fen water balance used the $w < 0$ form of Eq. (6) only once, at the end of September 2003, when the water table was 0.38 m below the average peat surface. On September 30, 2002 and for September 30, 2004–2009, the water table was above the average peat surface and no significant correction for water retention by the peat was necessary.

3.3.3. Surface energy balance

The net radiation flux density R_n was calculated from component measurements of upwelling and downwelling shortwave and longwave radiation. The three mature forest sites used paired pyranometers (model CM11, Kipp and Zonen, Delft, The Netherlands) and paired pyrgeometers (model PIR, Eppley Laboratory, Newport, RI, USA). The three harvested sites and the fen used a four-component net radiometer (model CNR1, Kipp and Zonen, Delft, The Netherlands). The upward-facing radiometers were mounted atop the scaffold flux tower in ventilated housings to minimize dew and frost on the sensor domes. The net radiometers and the downward-facing radiometers were mounted on a horizontal boom that extended 4 m to the south of the flux towers, 5–10 m above the forest canopies and 15 m above the Fen. The net radiometers were heated in winter to prevent frost formation on the sensor domes.

The soil heat flux Q_g was measured using four Middleton (Carter-Scott Design, Brunswick, Australia) model CN3 soil heat flux plates at 3-cm depth at OA and H02 and 10-cm depth at the other sites, corrected for the heat storage change in the soil layer above the flux plates. At the Fen, an additional term for heat storage in ponded water was added to Q_g, based on measured water temperature and depth. At the mature forest sites and H75, the biomass heat storage flux Q_b in the understory and tree boles, branches and foliage was estimated from six to fifteen measurements of tree bole temperature using 30-guage chromel-constantan thermocouples at several depths in the bole (McCaughey and Saxton, 1988; Blanken et al., 1997; Barr et al., 2006) and using the biomass estimates of Gower et al. (1997). Foliage, branch and understory temperatures were assumed to track in-canopy air temperatures. The photosynthetic energy flux Q_p was calculated from net ecosystem exchange (Blanken et al., 1997). Further details of the surface energy balance measurements are given in Barr et al. (2006).

Eddy-covariance measurements of H, λE, net ecosystem exchange and the friction velocity u_* were made from twin scaffold towers at approximately twice the height of the forest canopy and 4 m from the surface at the Fen. The surface fluxes were calculated as the sum of the eddy fluxes and the rate of change of storage in the air layer below the EC measurement (see Barr et al., 2006). The EC system consisted of a tri-axial sonic anemometer (model R3 or R3-50, Gill Instruments Ltd., Lymington, UK at OA, OBS and H75; model CSAT3, Campbell Scientific Inc., Logan, UT, USA at OJP, H02 and Fen; and model SAT-550, Kaijo Co., Tokyo, Japan at H94) in combination with an infrared gas analyzer. All sites but the Fen used a thermostated, closed-path, infrared gas (CO_2/H_2O) analyzer (model LI6262 or LI7000, LI-COR Inc., Lincoln, NE, USA) operated in absolute mode. A diaphragm pump was used to draw air into the IRGA at a flow rate of 10 l min^{-1}, through a 4-m long, 4-mm inner-diameter, heated tube (Synflex, 1300, Saint Gobain Performance Plastics, Wayne, NJ, USA). Additional details are given in Black et al. (1996) and Zha et al. (2009). The Fen used an open-path infrared gas (CO_2/H_2O) analyzer (model 7500, LI-COR Inc., Lincoln, NE, USA) (Sonnentag et al., 2009).

Nighttime fluxes were filtered using a site-specific u_* threshold (OA, OBS, OJP and H75: 0.35 m s^{-1}; H94 and Fen: 0.20 m s^{-1}; H02: 0.10 m s^{-1}). Gaps in H and λE were filled as described by Amiro

et al. (2006). The energy-closure fraction CF was computed annually from least-squares linear regression, forced through the origin, of 30-min $H + \lambda E$ versus $R_n - Q$. The analysis used data from the warm season only, when all the energy-balance terms were measured. CF was then used to calculate an energy-closure adjusted value for evapotranspiration E^* as

$$E^* = \frac{E}{\mathrm{CF}} \tag{7a}$$

which forces energy balance closure while preserving the measured Bowen ratio ($\beta = H/\lambda E$) (Blanken et al., 1997; Twine et al., 2000; Wohlfahrt et al., 2010). Eq. (7a) was applied in two ways: using annual, site-specific estimates of CF or the overall CF mean (0.85). The rationale behind using a single mean CF for all sites and years was that the uncertainty of the annual estimates was similar to the variability among sites and years. The resulting differences in E from the two approaches (mean versus site-year specific CF) were relatively small when integrated over the period of record. On an annual basis, they provide insight into the impact of the uncertainty in CF on E^* and therefore O^*.

In addition to Eq. (7a), we used a second energy-closure-adjustment scheme that allows the flux deficit to have a different Bowen ratio than the measured fluxes. Assuming that the measured fluxes have a Bowen ratio of β and that the "missing" fluxes have a Bowen ratio of $\gamma\beta$, we find:

$$E^* = E\left[1 + \frac{(\beta+1)(1-\mathrm{CF})}{(\gamma\beta+1)\mathrm{CF}}\right] \tag{7b}$$

The partitioning factor γ characterizes the relative susceptibilities of H and λE to under-measurement. A γ value of less than one indicates that H contributes proportionally less than λE to the flux deficit. Eq. (7b) forces energy-balance closure, setting the Bowen ratio of the "missing" fluxes to $\gamma\beta$.

3.3.4. Vertical water balance

Streamflow data for the White Gull Creek watershed were obtained from the Water Survey of Canada (WSC station 05KE010, 53.86°N, 104.62°W). Stand-level outflow O at each flux tower was calculated annually for the October to September hydrologic year as

$$O = P - E - \Delta S \tag{8}$$

Energy-closure adjusted values for O (which will denote as O^*) were also calculated by substituting E^* for E in Eq. (8).

Stand-level O from the seven flux towers was scaled from stand to watershed as the area-weighted average of five land-cover types (aspen, black spruce, jack pine, harvested jack pine and fen)

$$\bar{O} = \sum_{i=1}^{n} f_i O_i \tag{9}$$

where $\bar{O}$ is the area-weighted average and f_i is the land-cover type's area fraction (Table 1). $\bar{O}$ was also calculated as $\bar{O}^*$ based on O^*, i.e., with energy-closure adjustments to E. Because the harvested sites were not active during the entire integration period (2002–2009), missing annual values of O and O^* were infilled based on the mean ratio between the site and OJP during overlapping years.

3.3.5. Uncertainty

In order to compare estimated watershed outflow ($\bar{O}$ and $\bar{O}^*$) with measured streamflow F, we attempted to quantify random uncertainties in each of these terms, as well as to identify possible sources of systematic uncertainty. The random uncertainty in measured streamflow was estimated conservatively as 15% of annual F (Jeff Woodward, Water Survey of Canada, personal communication). The uncertainties in $\bar{O}$ and $\bar{O}^*$ arose from two sources:

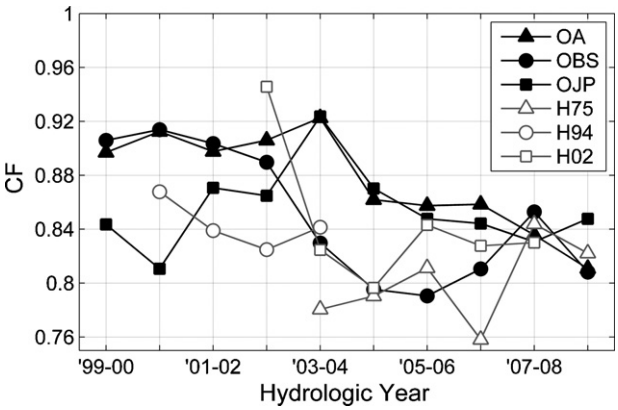

Fig. 3. Annual warm-season energy-balance-closure fraction CF for six flux-tower sites, October–September hydrologic years, 1999–2009.

measurement uncertainties in P, E, E^*, ΔS and f (Eqs. (8) and (9)); and scaling uncertainty related to the representativeness of the sites and measurements. We did not attempt to quantify the scaling uncertainty except as related to the uncertainty in the land-cover-type fractions (Table 1, Eq. (9)). Random uncertainties were estimated for all terms in Eqs. (8) and (9), although some uncertainties were estimated with greater rigour than others. Random uncertainties in annual E and E^* were estimated by adapting the framework of Richardson et al. (2006, 2007) to λE, using the Fluxnet-Canada gap-filling method to fill gaps in λE (Amiro et al., 2006). The analysis produced random uncertainties (95% confidence intervals) in annual E and E^* that varied between 1.2% and 2.9% of the annual totals. All other random uncertainties were estimated as fractions. The random uncertainties were set conservatively 5% of annual P, 10% of annual ΔS and 50% of the land-cover-type fractions f. The random uncertainties were combined in quadrature, both in estimating the uncertainties in O and O^* for each land-cover type (Eq. (8)) and in scaling these uncertainties to the watershed (Eq. (9)). The assessment of systematic uncertainty was largely qualitative (Section 5.1).

4. Results

4.1. Energy-balance closure

Fig. 3 shows annual energy-closure fractions for the BERMS forest sites, based on the warm season when the measurements fully resolved the surface energy storage fluxes. Annual CF varied from 0.76 to 0.95, with a mean (S.D.) of 0.85 (0.04) across all sites and years. Differences in CF were larger among years at one site than among sites. At the Fen, CF was more difficult to assess; the best analysis, which gave an overall mean of 0.81, focused on periods with ponded water of known depth. A more detailed energy-closure analysis at the three long-term sites is given in Barr et al. (2006).

Energy-balance closure did not improve when CF was estimated based on the long-term, cumulative sums of $H + \lambda E$ and $R_n - Q$ (Amiro, 2009). The cumulative analysis used 10 years of data from complete annual cycles at the mature forest sites. It assumed that, over this period, all components of Q became negligibly small except for one – the heat flux required for snow melt, which was calculated to be about 2.2% of R_n. The resulting ratios of cumulative $H + \lambda E$ to cumulative $R_n - Q$, integrated over 10 hydrologic years (1999–2009), were 0.81 (OA), 0.78 (OBS) and 0.87 (OJP). These values are slightly lower than the annual, warm-season CF values in Fig. 3, which averaged to 0.85. The reason for the difference is unknown; the difference suggests that the eddy-covariance CF may

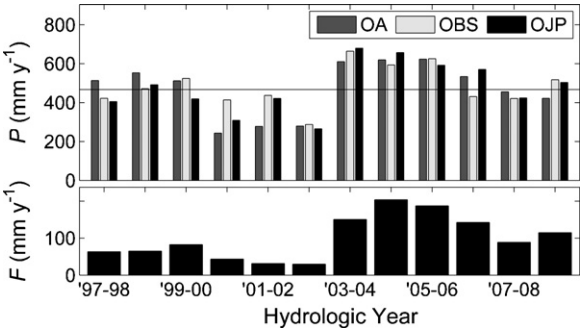

Fig. 4. Annual precipitation P for the long-term BERMS flux towers (upper panel); annual measured streamflow F for the White Gull Creek watershed (lower panel), October–September hydrologic years, 1997–2009. The horizontal line in the upper panel shows the 1971–2000 mean annual P (467 mm) from the Waskesiu climate station.

be smaller in the cold season than the warm season, but we do not have the data to verify this empirically.

4.2. Stand-level water balance

Figs. 4–6 and Table 3 show components of the vertical water balance for each of the seven flux towers. The study period (1999–2009) was characterized by extreme contrasts in annual precipitation and streamflow, with three years of drought (2001–2003) followed by three years of extreme wet weather (2004–2006). The large inter-site differences in annual P during some years reflect the high spatial variability of summer convective precipitation. Compared to the 1971–2000 climatic normals for mean (S.D.) annual P (Waskesiu Lake: 467 (87) mm; Prince Albert Airport, 53.22°N, 105.67°W: 424 (67) mm; Nipawin Airport, 53.22°N, 105.67°W: 440 (62) mm; La Ronge Airport, 53.22°N, 105.67°W: 483 (73) mm), the 1999–2009 study period had near normal mean annual P but with above-normal variability (OA 458 (148) mm; OBS 491 (115) mm; 484 (141) OJP). Note that the measurements at the harvested sites were limited in duration and were made during a period of above-normal P. This limitation complicates the direct comparison of the water balance among sites.

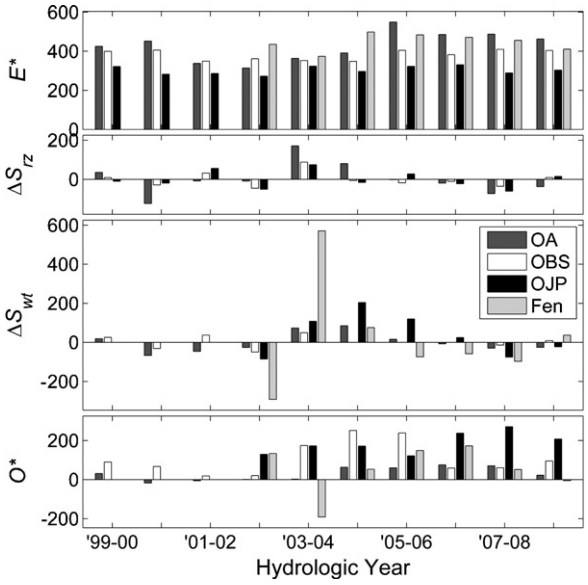

Fig. 5. Components of the annual water balance at the three mature forest and fen sites, October–September hydrologic years, 1999–2009.

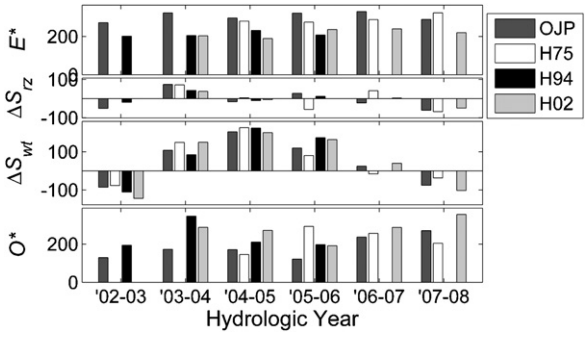

Fig. 6. Components of the annual water balance at the four jack pine sites, October–September hydrologic years, 2002–2008.

Measured streamflow F from the White Gull Creek watershed tracked the temporal pattern in P but with amplified inter-annual variability (Fig. 4, lower panel). The ratio of F to P (based on P from OBS and OJP) had a mean of 0.21 for 1997–2009, with annual F/P ratios that ranged from 0.07 during the drought (2001–2002) to 0.33 during the wet period that followed the drought (2004–2005).

Evapotranspiration varied by a factor of two among sites, with the highest mean annual E^* at the fen, aspen and black spruce sites, intermediate E^* at the mature and mid-aged jack pine sites, and the lowest E^* at the two young jack pine stands (Table 2). Among years at each site, annual E^* was relatively constant, despite the high inter-annual variability in P, with coefficients of variation CV of 0.07–0.10 at all sites but OA. The higher CV in annual E^* at OA (0.18) reflected the high sensitivity of this site to inter-annual climatic variability and drought (Zha et al., 2010).

The annual water-balance storage changes associated with root-zone soil water and water table depth were large for some site-years, with inter-annual variability comparable to that of P (Table 3). At the two sites with 10 years of record (OA and OBS), however, the ΔS mean was near zero; in most circumstances, mean annual ΔS should tend to zero over long periods. The other five sites had positive mean ΔS associated with a rising water table, reflecting the above-normal P of their study years. Of particular note are: the extreme inter-annual variability in ΔS at the Fen; the low inter-annual variability in ΔS at OBS; and the high inter-annual variability in the water-table component ΔS_{wt} at the jack pine sites. At the jack pine sites, changes of water content in the unsaturated zone between the water table and the bottom of the root zone (taken to be 2.5 m) were assumed to be negligible, but this assumption could introduce some error in the estimate of year-to-year storage changes when the vertical flux has changed.

The estimates of stand-level outflow, calculated as water balance residuals (Eq. (8)) were sensitive to the energy-closure adjustment to E. The energy-closure adjustment to E decreased outflow by 68% at OA, 54% at Fen and between 10% and 35% at OBS and the jack pine sites. This is not surprising given the magnitude of the adjustment to E (+18%, or 28–82 mm y^{-1} across all site-years). The question of closure is addressed in Sections 4.3 and 5.1. Regardless of energy-closure adjustments, the aspen and fen sites had the lowest outflows, the black spruce site had intermediate outflow, and the jack pine and especially the younger jack pine sites had the highest outflows. However, the outflow estimates may not typify the long-term means, particularly at the young jack pine sites, because of the limited number of years in this analysis.

4.3. Estimated outflow in relation to measured streamflow

Figs. 7 and 8 and Table 4 compare measured streamflow F from the White Gull Creek watershed with flux-tower-based estimates of watershed outflow $\bar{O}$ and $\bar{O}^*$ from Eq. (9), computed as

Table 3
Annual mean (S.D.) components of the vertical, stand-level water balance by site: precipitation P, energy-closure-adjusted evapotranspiration E^*, soil water storage ΔS, and outflow (Eq. (8), with (O^*) or without (O) energy-closure adjustments to E). The closure-adjustment to E used Eq. (7a) with CF = 0.85. The values are restricted to years with complete measurements, so that the study years vary among sites.

Site	Period[a]	P (mm y^{-1})	E^* (mm y^{-1})	ΔS_{rz} (mm y^{-1})	ΔS_{wt} (mm y^{-1})	ΔS (mm y^{-1})	O (mm y^{-1})	O^* (mm y^{-1})
Old Aspen	1999–2009	458 (148)	427 (74)	2 (81)	−1 (50)	1 (128)	94 (43)	30 (35)
Fen	2002–2009	522 (158)	447 (44)	n/a	n/a	23 (269)	119 (130)	52 (125)
Old Black Spruce	1999–2009	491 (115)	382 (26)	−1 (39)	3 (30)	2 (67)	165 (84)	108 (85)
Old Jack Pine	2002–2009	527 (145)	306 (21)	−5 (47)	39 (109)	34 (141)	233 (55)	187 (55)
Harvested, 1975	2004–2008	561 (98)	292 (22)	−20 (52)	64 (120)	44 (139)	269 (63)	225 (64)
Harvested, 1994	2002–2006	549 (192)	212 (14)	7 (28)	93 (148)	100 (157)	269 (73)	237 (73)
Harvested, 2002	2003–2008	585 (100)	218 (21)	−3 (31)	90 (123)	88 (147)	312 (58)	279 (59)

[a] Hydrologic years, beginning October 1 of the first year and ending September 30 of the final year.

Table 4
Mean (S.D.) annual outflow $\bar{O}$ and $\bar{O}^*$ (mm y^{-1}) from the White Gull Creek watershed, calculated as an area-weighted average of stand-level outflow at the BERMS flux towers (Eq. (9)) or at the OBS site alone, in relation to measured streamflow F (mm y^{-1}). Stand-level outflow was estimated without (O) and with (O^*) energy-closure adjustments to E. The three estimates for watershed outflow $\bar{O}^*$ were based on E^* from three energy-closure adjustment schemes: Eq. (7a) with different CF for each site-year; Eq. (7a) with mean CF of 0.85; and Eq. (7b) with CF of 0.85 and γ of 0.5.

Scaling approach	Period[a]	$\bar{O}$	$\bar{O}^*$ (based on E^* from Eq. (7a), annual CF)	$\bar{O}^*$ (based on E^* from Eq. (7a), CF = 0.85)	$\bar{O}^*$ (based on E^* from Eq. (7b), CF = 0.85, γ = 0.5)	F
All sites (Eq. (9))	2002–2009	182 (40)	112 (30)	127 (37)	109 (36)	131 (60)
OBS site only	1999–2009	165 (84)	100 (70)	108 (85)	87 (85)	107 (63)

[a] Hydrologic years, beginning October 1 of the first year and ending September 30 of the final year.

area-weighted averages of the contributions from five land cover types. Also shown in Fig. 7 and Table 4 are O^* estimates from the OBS site alone, assuming that OBS represents the whole watershed. Table 4 includes four tower-based estimates: $\bar{O}$ computed without energy-closure adjustments to E, and $\bar{O}^*$ computed with energy-closure adjustments to E from three different adjustment schemes. For all three adjustment schemes, $\bar{O}^*$, with energy-closure adjustments, agreed more closely with F than did $\bar{O}$, which lacked energy-closure adjustments. The differences are striking. Whereas estimated $\bar{O}$ exceeded F by ~40%, mean $\bar{O}^*$ and F agreed to within 15%. The random uncertainty limits for cumulative outflow from October 2002 to September 2009 (Fig. 8) show overlap between F and $\bar{O}^*$ but separation of F from $\bar{O}$. Even on an annual basis (Fig. 7), all three estimates of outflow were significantly and positively related to F (e.g., $\bar{O}^* = 60\,\text{mm y}^{-1} + 0.51F$, $r^2 = 0.69$, $p = 0.02$), with two caveats: both $\bar{O}$ and $\bar{O}^*$ had lower inter-annual variability than F; and the slopes (±95% confidence intervals) of the $\bar{O}$ versus F (0.54 ± 0.34) and $\bar{O}^*$ versus F (0.51 ± 0.39) relationships were significantly less than one.

5. Discussion

5.1. Energy- and water-balance closure

The application of energy-closure adjustments to evapotranspiration improved the agreement between measured streamflow and flux-tower-based estimates of watershed outflow. This result supports the use of energy-closure adjustments to correct a systematic bias in E, albeit with some uncertainty as to their magnitude and implementation (Section 5.2). In an earlier study of the same watershed spanning 1994–1996, Nijssen and Lettenmaier (2002) found a similar discrepancy between measured streamflow and scaled outflow estimated using a simple evapotranspiration model that was tuned to the data from five flux towers, without energy-closure adjustments to E. These results contrast with two similar studies that compared the water balance at flux towers with gauged streamflow from much smaller (<1 km^2) catchments. Wilson et al. (2001) reported good agreement between unadjusted

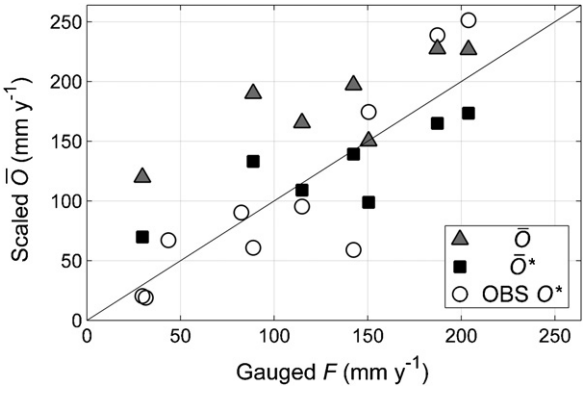

Fig. 7. Estimated annual watershed outflow $\bar{O}^{(*)}$ in relation to measured streamflow from the White Gull Creek watershed. Outflow O was estimated as a water-balance residual at the flux towers then scaled from stand to watershed using area-weighted averaging. Included are three estimates of outflow: $\bar{O}$ and $\bar{O}^*$ (2002–2009), estimated from Eq. (9) without and with energy-closure adjustments to E (CF = 0.85); and O^* (1999–2009) from the OBS site alone (CF = 0.85).

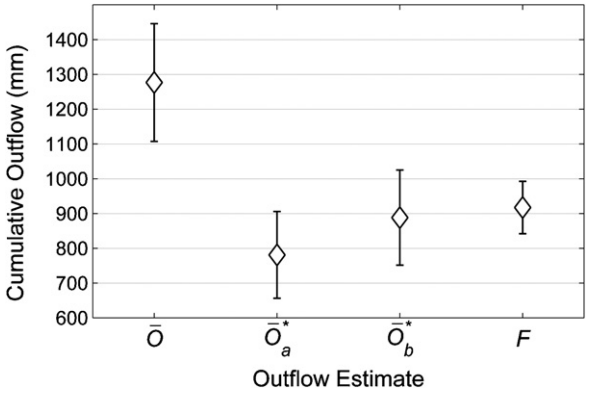

Fig. 8. Four estimates of cumulative outflow from the White Gull Creek watershed, October 2002 to September 2009: estimated outflow scaled from stand to watershed based on the vertical water balance at seven flux towers, without ($\bar{O}$) and with energy-closure adjustments to E ($\bar{O}^*_a$ using site-specific, annual CF; $\bar{O}^*_b$ using CF = 0.85); and measured streamflow F. The error bars show the random uncertainties (Section 3.3.5).

eddy-covariance measurements of E and catchment-scale E estimated as a water balance residual. The results of Scott (2010) were less conclusive; closure adjustments to E improved water-balance closure in two of three small catchments when integrated over multiple years but worsened annual water-balance closure. The more definitive conclusions from this study may be related to the larger catchment area (603 km^2), which minimized the possibility that lateral outflow through the watershed boundaries was a significant component of streamflow.

Given the uncertainties in the individual terms needed to estimate CF and $\bar{O}^*$ including the various components of the energy and water balances (Eqs. (1) and (2a)), the close agreement between $\bar{O}^*$ and F in Table 4 is remarkable. Nevertheless, it is unlikely that the difference between $\bar{O}$ and F (1277 mm versus 917 mm, accumulated from October 2002 to September 2009) can be explained by undetected systematic errors in F, ΔS, land-cover-type fraction or P. A −30% bias in F is implausible. ΔS becomes small when averaged over multiple years so that any measurement biases must also become small. Uncertainties in the land-cover-type fractions (Eq. (9)) have only moderate impact on area-weighted outflow, in part because the differences in E among land-cover types are relatively small.

More plausible is a bias in P. Many studies have reported under-measurement by accumulating precipitation gauges of 4–6% for rainfall and 30% or more for snowfall (e.g., Legates and DeLiberty, 1993; Sevruk et al., 2009). However, these studies concluded that P under-measurement can be minimized through gauge design, optimal siting and the use of empirical corrections for wind-induced undercatch. In this study, we minimized systematic uncertainties in P by deploying shielded accumulating gauges in small forest clearings in near-optimal conditions to maximize catch efficiency (Barry Goodison, personal communication), and by applying empirical corrections for snowfall undercatch. Moreover, in order for a systematic error in P to account for the observed discrepancy between $\bar{O}$ and F, P would need to be biased high (not low) by about 10%, which in unlikely.

The flux-tower-based estimates of watershed outflow $\bar{O}$ and $\bar{O}^*$ could be compromised by the limited spatial coverage of the precipitation gauges. There are two issues: the limited number of gauges; and the lack of coverage in the northern half of the watershed. Concerning the latter, the 1971–2000 climate normals from eight class-A reference climate stations in central Saskatchewan (www.climate.weatheroffice.gc.ca) showed a slight north–south gradient in P (+28 mm y^{-1} per degree increase in latitude). Given the dimensions of the watershed and the southerly locations of the flux towers, this north–south gradient suggests that the flux towers may have underestimated mean P for the watershed, but only slightly, by ~2 mm y^{-1}. Concerning the limited number of P gauges, Eq. (9) effectively weights the four gauges by their site's respective land-cover-type fractions; OBS and OJP (which are within the watershed near its western and south-eastern boundaries) and OA and Fen (which lie outside the watershed) are weighted, respectively, by: 0.39, 0.29 (including the harvested sites), 0.18 and 0.14. Three observations increase our confidence that the four gauges provide an adequate estimate of watershed mean P: (1) the P measurements from the two gauges within the watershed were given the highest weightings; (2) mean annual P during the October 2002 to September 2009 analysis period was quite uniform across sites (OA 507, OBS 506, OJP 527 and Fen 522 mm y^{-1}); and (3) the two P measurements from outside the watershed (OA and Fen) were comparable to those within (OBS and OJP). Averaged over the seven-year analysis period, the P variability among measurements (range 22 mm y^{-1}) was small compared with the $\bar{O}$ versus F discrepancy (51 mm y^{-1}).

On the other hand, it is very plausible that the measurements of E are biased low and that this bias is responsible for the observed discrepancy between $\bar{O}$ and F. The magnitude of the $\bar{O}$ versus F discrepancy is consistent with the observed energy imbalance. The comparison hinges on the accuracy of the surface available energy measurement. Twine et al. (2000) estimated the uncertainty in surface available energy to be 10%. However, it is unlikely that the measurements of surface available energy have a significant systematic bias, because of the quality of the R_n measurements and because Q becomes small when averaged over long periods. All evidence points to a systematic bias in E. Eddy-covariance measurement deficits in E have also been found in lysimeter studies of the vertical water balance (Barr et al., 2000; Wohlfahrt et al., 2010).

The evaluation of energy and water balance closure places high demands on the data. Three factors reduced the uncertainties in this study and contributed to the agreement between F and $\bar{O}^*$: the analysis of multiple years of data from multiple sites, which reduced the random uncertainties in the area-weighted means; the tendency of ΔS to become small when averaged over many years; and the careful design of the measurement systems to eliminate systematic errors. The design features included: use of high-quality radiometers with frequent calibration and no signs of calibration drift; careful measurement of the surface energy storage fluxes; use of closed-path, short-tube eddy-covariance systems with high flow rates through temperature-controlled gas analyzers; careful processing and quality assurance of the eddy-covariance data; use of accumulating precipitation gauges located in small forest clearings in near-optimal conditions to minimize undercatch; complete measurements of soil water storage including root-zone water content and water table depth; and frequent maintenance of the streamflow gauge.

The observed energy closure fractions (0.85 ± 0.04) are comparable to previous studies but with greater consistency among sites and years. Foken (2008) compiled energy-closure data over short vegetation and reported CF of 0.63–0.90. Wilson et al. (2002) found somewhat larger differences among 22 FLUXNET sites, with CF ranging from 0.56 to 0.97. The differences between these studies and our study may be in the nature of the sites or the uniformity of the measurements. The sites in this study were all continental, with level topography and uniform fetch; all had high-quality measurements of surface available energy; and all used standardized eddy-covariance instrumentation and data-processing software.

5.2. Energy-closure adjustments

Although the energy-closure analysis produced robust estimates of the energy-closure fraction CF (Eq. (3)), it does not provide any guidance about how the energy imbalance ε is partitioned between H and λE. The most common energy-closure adjustment scheme (Eq. (7a)) assumes that the partitioning is proportional, multiplying both H and λE by a factor of CF^{-1} and thus preserving the measured Bowen ratio (Twine et al., 2000; Barr et al., 2006; Wohlfahrt et al., 2010). Given the absence of other information, this approach is the most reasonable.

However, Barr et al. (2006) give evidence that the measured and "missing" fluxes may have different Bowen ratios, based on data from the deciduous OA site in this study. The CF at OA varied seasonally, with higher CF during leafless periods when the Bowen ratio was high and lower CF during fully leafed periods when the Bowen ratio was low. The analysis suggested that λE was twice as prone as H to under-measurement. The difference could be caused by differences in the frequency responses of temperature and humidity measurements, related, e.g., to the time constant of the infrared gas analyzer or the dampening of the water vapour fluctuations within the sampling tube (Leuning and Moncrieff, 1990). It could also have micrometeorological causes (e.g., Katul and Hsieh, 1999). To allow for different Bowen ratios between the measured and "missing"

fluxes, we implemented an alternate energy-closure adjustment scheme (Eq. (7b)), using γ of 0.5 (Barr et al., 2006) and CF of 0.85 across all sites and years. A γ value of 0.5 indicates that λE is twice as prone as H to under-measurement. The use of Eq. (7b) instead of (7a) increased the effective closure adjustment to E from +18% at all sites, based on the mean CF of 0.85, to +20% at Fen, +22% at OA, +24% at OBS and +25–26% at the jack pine sites. In turn, these increases in E^* caused a reduction in area-averaged $\bar{O}^*$ (2002–2009) from 127 to 109 mm y^{-1} compared with measured streamflow of 131 mm y^{-1}. Because the uncertainties are large, we cannot draw a definite conclusion about which energy-closure adjustment scheme is better. However, the comparison tentatively favours the simpler scheme (Eq. (7a)). If the flux measurement deficit is caused by limitations in the angle of attack operating range of the sonic anemometers, as reported by Nakai et al. (2006), then the relative impacts on H and λE will be similar and Eq. (7a) will be the more appropriate adjustment scheme.

Given the magnitude of the energy imbalance in this and other studies, we recommend caution in estimating evapotranspiration as an energy-balance residual (i.e., as $E = R_n - H - Q$) (Amiro, 2009). The primary weakness of the energy-balance residual method is that measurement deficits in H are attributed to λE. When applied in this study, the residual method increased mean annual E by 173 mm y^{-1}, resulting in a slightly negative estimate for watershed outflow. Without prior knowledge of the energy-closure fraction, it is impossible to estimate the flux deficit or partition the deficit between H and λE.

5.3. Implications for the hydrology of the boreal forest

The long-term ratio of streamflow to precipitation for this watershed was 0.21, with large differences among years (0.07–0.33) and large contrasts among the outflow contributions from different land-cover types. The watershed is typical of the southern Boreal Plains ecozone. Different land-cover types have fundamentally different hydrologic regimes. Aspen forests have a characteristically low outflow, with values that range from zero during dry years to 75 mm y^{-1} during wet years. Over the long-term, the aspen forests transpire most of the precipitation that they receive (Blanken et al., 2001). In contrast, the sandy, upland jack pine forests maintain a relatively high outflow (122–270 mm y^{-1}) during both wet and dry years. Their permeable soils and deep water tables promote drainage away from the root zone even during years of low total P.

Most hydrologically dynamic are the wetland fens and the lowland black spruce forests. The black spruce stands, which are found in moderate topographic depressions with high water tables, have high outflow (up to 250 mm y^{-1}) during wet years and low outflow (20 mm y^{-1}) during dry years. The water table responds sensitively to $P - E^*$ but the amplitude of its fluctuations is limited. Periods of excess $P - E^*$ raise the local water table to near the surface and promote lateral outflow, whereas periods of deficit $P - E^*$ cause the local water table to drop, restricting lateral outflow. The black spruce forests typify the boreal forest landscape hydrologically, with annual outflow that is similar to the landscape mean. The wetland fens are even more dynamic, with large and bidirectional lateral exchange with the surrounding uplands, primarily via the groundwater. The fens have huge storage capacity, absorbing water from the surrounding uplands during wet years but releasing water to the uplands during dry years. The result is low mean outflow ($\sim$50 mm y^{-1}) but with large inter-annual variability (ranging from −191 to +172 mm y^{-1}).

The hydrology of the Boreal Plains ecozone is complex because of its low but variable outflow, subtle topography, diversity of vegetation types, and frequent disturbance by wildfire and harvesting. The coherence of the water balance analysis at stand and watershed scales in this study underscores the value of co-locating flux-towers and gauged catchments (Sellers et al., 1997; Scott, 2010). The co-location of stand-level measurements of the energy and water balances with watershed-scale measurements of streamflow provides a broad perspective for understanding hydrological processes and a dual constraint for evaluating and improving hydrological models (Nijssen and Lettenmaier, 2002).

6. Summary and conclusions

This study revisits the question of energy-balance closure by the eddy-covariance method, using streamflow measurements to provide an independent constraint on the vertical water balance at flux towers. Stand-level outflow from seven proximate flux towers in the southern boreal forest was estimated as a residual term in the vertical water balance, then scaled to the watershed by area-weighted averaging based on land-cover-type fraction. The watershed outflow was then compared with measured streamflow from a gauged watershed within the study area, over a seven-year period (2002–2009).

On average, the flux-tower measurements of H and λE underestimated surface available energy ($R_n - Q$) by 15%. The annual energy-closure fraction CF was similar across sites and years, with an overall mean (S.D.) of 0.85 (0.04). Differences among years at one site were comparable to differences among sites. Based on the energy-closure analysis, closure-adjusted values of evapotranspiration E^* were calculated as E/CF.

Stand-level estimates of outflow at the flux towers were sensitive to the use of energy-closure adjustments to E, declining by an average of 28% (52 mm y^{-1}) when adjustments were applied. When scaled to the watershed, the tower-based estimates of outflow $\bar{O}$ and $\bar{O}^*$ agreed with measured streamflow F only when outflow was estimated with energy-closure adjustments to E. Without energy-closure adjustments, $\bar{O}$ exceeded F by 40%, which was greater than the random uncertainties in $\bar{O}$ and F. With energy-closure adjustments to E, $\bar{O}^*$ and F agreed to within 15%. The independent assessment of the water and energy balances at the watershed scale thus provided support for the use of energy-closure adjustments to E.

Streamflow from the southern Boreal Plains watershed in this study had a long-term mean of 101 mm y^{-1}, about 20% of precipitation. However, it was highly variable, both among years, ranging from 30 mm y^{-1} during the 2001–2002 drought to 204 mm y^{-1} during the excessively wet 2004–2005 period, and with respect to the contributions from different land-cover types. Stand-level outflow varied from 30 mm y^{-1} at the mature aspen forest and 52 mm y^{-1} at the fen to 108 mm y^{-1} at the mature black spruce forest and 187 and 250 mm y^{-1} at the mature and young (harvested) jack pine forests, respectively. The dominant land-cover type, mature black spruce forest, typified the hydrology of the boreal forest landscape, with intermediate outflow that was similar to the watershed mean.

Acknowledgements

We gratefully acknowledge the work of Joe Eley, Dell Bayne, Charmaine Hrynkiw, Erin Thompson, Craig Smith, and Steve Enns, who oversaw the meteorological measurements and data management; Randy Schmidt, who installed and operated the water table wells; Andrew Sauter, Rick Ketler, Dominique Lessard, Dave Wieder, Dan Finch and Sheila McQueen, who provided laboratory, field and data management support for the flux measurements; and Barry Goodison and Bob Stewart, who championed the BERMS program. Financial support was provided by the Climate Research Branch of Environment Canada, the Canadian Forest Service, Parks Canada, the Action Plan 2000 on Climate Change, the Program

of Energy Research and Development, the Climate Change Action Fund, the Natural Sciences and Engineering Research Council of Canada, the Canadian Foundation for Climate and Atmospheric Science, BIOCAP Canada, and the National Aeronautic and Space Administration.

References

Amiro, B.D., Barr, A.G., Black, T.A., Iwashita, H., Kljun, N., McCaughey, J.H., Morgenstern, K., Murayama, S., Nesic, Z., Orchansky, A.L., Saigusa, N., 2006. Carbon, energy and water fluxes at mature and disturbed forest sites, Saskatchewan, Canada. Agric. Forest Meteorol. 136, 237–251.

Amiro, B., 2009. Measuring boreal forest evapotranspiration using the energy balance residual. J. Hydrol. 366, 112–118.

Aubinet, M., Grelle, A., Ibrom, A., Rannik, Ü., Moncrieff, J., Foken, T., Kowalski, A.S., Martin, P.H., Berbigier, P., Bernhofer, Ch., Clement, R., Elbers, J., Granier, A., Grünwald, T., Morgenstern, K., Pilegaard, K., Rebmann, C., Snijders, W., Valentini, R., Vesala, T., 2000. Estimates of the annual net carbon and water exchange of European forests: the EUROFLUX methodology. Adv. Ecol. Res. 30, 114–175.

Barr, A.G., van der Kamp, G., Schmidt, R., Black, T.A., 2000. Monitoring the moisture balance of a boreal aspen forest using a deep groundwater piezometer. Agric. Forest Meteorol. 102, 13–24.

Barr, A.G., Betts, A.K., Black, T.A., McCaughey, J.H., Smith, C.D., 2001. Intercomparison of BOREAS northern and southern study area surface fluxes in 1994. J. Geophys. Res. 106, 33,543–33,550.

Barr, A.G., Morgenstern, K., Black, T.A., McCaughey, J.H., Nesic, Z., 2006. Surface energy balance closure by the eddy-covariance method above three boreal forest stands and implications for the measurement of the CO_2 flux. Agric. Forest Meteorol. 140, 322–337.

Black, T.A., den Hartog, G., Neumann, H.H., Blanken, P.D., Yang, P.C., Russel, C., Nesic, Z., Lee, X., Chen, S.G., Staebler, R., Novak, M.D., 1996. Annual cycles of water vapor and carbon dioxide fluxes in and above a boreal aspen forest. Global Change Biol. 2, 219–229.

Blanken, P.D., Black, T.A., Yang, P.C., Neumann, H.H., Nesic, Z., Staebler, R., 1997. Energy balance and canopy conductance of a boreal aspen forest: Partitioning overstory and understory components. J. Geophys. Res. 102, 28,915–28,927.

Blanken, P.D., Black, T.A., Neumann, H., den Hartog, G., Yang, P.C., Nesic, Z., Lee, X., 2001. The seasonal water and energy exchange above and within a boreal aspen forest. J. Hydrol. 245, 118–136.

Bonan, G.B., Shugart, H.H., 1989. Environmental factors and ecological processes in boreal forests. Annu. Rev. Ecol. Syst. 20, 1–28.

Devito, K.J., Creed, I., Gan, T., Mendoza, C., Petrone, R., Silins, U., Smerdon, B., 2005. A framework for broad scale classification of hydrologic response units on the Boreal Plain: is topography the last thing to consider? Hydrol. Process. 19, 1705–1714.

Foken, T., 2008. The energy balance closure problem—an overview. Ecol. Appl. 18, 1351–1367.

Foken, T., Mauder, M., Liebethal, C., Wimmer, F., Beyrich, F., Leps, J.-P., Raasch, S., DeBruin, H.A.R., Meijninger, W.M.L., Bange, J., 2010. Energy balance closure for the LITFASS-2003 experiment. Theor. Appl. Climatol. 101, 149–160, doi:10.1007/s00704-009-0216-8.

Gower, S.T., Vogel, J.G., Norman, J.M., Kucharick, C.J., Steele, S.J., Sow, T.K., 1997. Carbon distribution and above ground net primary production in aspen, jack pine, and black spruce stands in Saskatchewan and Manitoba, Canada. J. Geophys. Res. 102 (D24), 29,029–29,041.

Goodison, B.E., 1978. Accuracy of Canadian snow gage measurements. J. Appl. Meteorol. 17, 1542–1548.

Grant, R., 2004. Modeling topographic effects on net ecosystem productivity of boreal black spruce forests. Tree Physiol. 24, 1–18.

Hogan, J.M., 2005. Hydrologic behavior and hydraulic properties of a patterned fen in Saskatchewan. M.Sc. thesis, University of Saskatchewan, Saskatoon, Saskatchewan, 107 pp.

Hogan, J.M., van der Kamp, G., Barbour, S.L., Schmidt, R., 2006. Potential field methods for measuring hydraulic properties of peat deposits. Hydrol. Process. 20, 3,635–3,649, doi:10.1002/hyp.6379.

Hogg, E.H., 1997. Temporal scaling of moisture and the forest-grassland boundary in western Canada. Agric. Forest Meteorol. 84, 115–122.

Ju, W., Chen, J.M., Black, T.A., Barr, A.G., McCaughey, J.H., Roulet, N., 2006. Hydrological effects on carbon cycles of Canada's forests and wetlands. Tellus B 58, 16–30.

Judd-Henrey, I., van der Kamp, G., Wismer, M., Rodriguez-Prado, A., 2008. Assessment of ground and surface water conditions in the Prince Albert Model Forest Area. Saskatchewan Research Council Publication No. 11618-1E08, 47 pp.

Katul, G.G., Hsieh, C.I., 1999. A note on the flux-variance similarity relationships for heat and water vapour in the unstable atmospheric surface layer. Boundary-Layer Meteorol. 90, 327–338, doi:10.1023/A:1001747925158.

Kidston, J., Brümmer, C., Black, T.A., Morgenstern, K., Nesic, Z., McCaughey, J.H., Barr, A.G., 2010. Energy balance closure using eddy covariance above two different land surfaces and implications for CO_2 flux measurements. Boundary-Layer Meteorol. 136, 193–218.

Landsberg, J.J., Gower, S.T., 1997. Applications of Physiological Ecology to Forest Management. Academic Press, Toronto.

Legates, D.R., DeLiberty, T.L., 1993. Precipitation measurement biases in the United States. J. Am. Water Resour. Assoc. 29, 855–861, doi:10.1111/j.1752-1688.1993.tb03245.x.

Leuning, R., Moncrieff, J., 1990. Eddy-covariance CO_2 flux measurements using open- and closed-path CO_2 analysers: corrections for analyser water vapour sensitivity and damping of fluctuations in air sampling tubes. Boundary-Layer Meteorol. 53, 63–76, doi:10.1007/BF00122463.

Li, Z.Q., Yu, G.R., Wen, X.F., Zhang, L.M., Re, C.Y., Fu, Y.L., 2005. Energy balance closure at ChinaFLUX sites. Sci. Chin. Ser. D – Earth Sci. 48, 51–62.

McCaughey, J.H., Saxton, W.L., 1988. Energy balance storage terms in a mixed forest. Agric. Forest Meteorol. 44, 1–18.

Nakai, T., van der Molen, M.K., Gash, J.H.C., Kodama, Y., 2006. Correction of sonic anemometer angle of attack errors. Agric. Forest Meteorol. 136, 19–30.

Nijssen, B., Lettenmaier, D.P., 2002. Water balance dynamics of a boreal forest watershed: White Gull basin, 1994–1996. Water Resour. Res. 38 (11), doi:10.1029/2001WR000699, issn: 0043-1397.

Oncley, S.P., Foken, T., Vogt, R., Kohsiek, W., DeBruin, H.A.R., Bernhofer, C., Christen, A., van Gorsel, E., Grantz, D., Feigenwinter, C., Lehner, I., Liebethal, C., Liu, H., Mauder, M., Pitacco, A., Ribeiro, L., Weidinger, T., 2007. The Energy Balance Experiment EBEX-2000, Part I: Overview and energy balance. Boundary-Layer Meteorol. 123, 1–28.

Richardson, A.D., Hollinger, D.Y., Burba, G.G., Davis, K.J., Flanagan, L.B., Katul, G.G., Munger, J.W., Ricciuto, D.M., Stoy, P.C., Suyker, A.E., Verma, S.B., Wofsy, S.C., 2006. A multi-site analysis of random error in tower-based measurements of carbon and energy fluxes. Agric. Forest Meteorol. 136, 1–18, doi:10.1016/j.agrformet.2006.01.00.

Richardson, A.D., Hollinger, D.Y., Aber, J., Ollinger, S.V., Braswell, B., 2007. Environmental variation is directly responsible for short- but not longterm variation in forest-atmosphere carbon exchange. Global Change Biol. 13, 788–803.

Scott, R.L., 2010. Using watershed water balance to evaluate the accuracy of eddy covariance evaporation measurements for three semiarid ecosystems. Agric. Forest Meteorol. 150, 219–225.

Sellers, P.J., Hall, F.G., Kelly, R.D., Black, A., Baldocchi, D., Berry, J., Ryan, M., Ranson, K.J., Crill, P.M., Lettenmaier, D.P., Margolis, H., Cihlar, J., Newcomer, J., Fitzjarrald, D., Jarvis, P.G., Gower, S.T., Halliwell, D., Williams, D., Goodison, B., Wickland, D.E., Guertin, F.E., 1997. BOREAS in 1997: experiment overview, scientific results and future directions. J. Geophys. Res. 102, 28,731–28,770.

Sevruk, B., Ondrás, M., Chvíla, B., 2009. The WMO precipitation measurement intercomparisons. Atmos. Res. 92, 376–380.

Sonnentag, O., van der Kamp, G., Barr, A., Chen, J., 2009. On the relationship between water table depth and water vapor and carbon dioxide fluxes in a minerotrophic fen. Global Change Biol., doi:10.1111/j.1365-2486.2009.02032.x.

Twine, T.E., Kustas, W.P., Norman, J.M., Cook, D.R., Houser, P.R., Meyers, T.P., Prueger, J.H., Starks, P.J., Wesely, M.L., 2000. Correcting eddy-covariance flux underestimates over a grassland. Agric. Forest Meteorol. 103, 279–3000.

van der Kamp, G., Hayashi, M., 2009. Groundwater-wetland ecosystem interaction in the semiarid glaciated plains of North America. Hydrogeology J. 17, 203–214.

Williams, M., Richardson, A.D., Reichstein, M., Stoy, P.C., Peylin, P., Verbeek, H., 2009. Improving land surface models with FLUXNET data. Biogeosciences 6, 1341–1359.

Wilson, K.B., Hanson, P.J., Mulholland, P.J., Baldocchi, D.D., Wullschleger, S.D., 2001. A comparison of methods for determining forest evapotranspiration and its components: sap-flow, soil water budget, eddy covariance and catchment water balance. Agric. Forest Meteorol. 106, 153–168.

Wilson, K., Goldstein, A., Falge, E., Aubinet, M., Baldocchi, D., Berbigier, P., Bernhofer, C., Ceulemans, R., Dolman, H., Field, C., Grelle, A., Ibrom, A., Law, B.E., Kowalski, A., Meyers, T., Moncrieff, J., Monson, R., Oechel, W., Tenhunen, J., Valentini, R., Verma, S., 2002. Energy balance closure at FLUXNET sites. Agric. Forest Meteorol. 113, 223–243.

Wohlfahrt, G., Irschick, C., Thalinger, B., Hörtnagl, L., Obojes, N., Hammerle, A., 2010. Insights from independent evapotranspiration estimates for closing the energy balance: a grassland case study. Vadose Zone J. 9, doi:10.2136/vzj2009.0158.

Zha, T.S., Barr, A.G., Black, T.A., McCaughey, J.H., Bhatti, J., Hawthorne, I., Krishnan, P., Kidston, J., Saigusa, N., Shashkov, A., Nesic, Z., 2009. Carbon sequestration in boreal jack pine stands following harvesting. Global Change Biol. 15, 1475–1487.

Zha, T.S., Barr, A.G., van der Kamp, G., Black, T.A., McCaughey, J.H., Flanagan, L.B., 2010. Interannual variation of evapotranspiration from forest and grassland ecosystems in western Canada in relation to drought. Agric. Forest Meteorol. 150, 1476–1484.